Journal of Materials and Environmental Sciences
ISSN : 2028-2508
CODEN : JMESCN

J. Mater. Environ. Sci., 2018, Volume 9, Issue 1, Page 334-344

https://doi.org/10.26872/jmes.2018.9.1.37

http://www.jmaterenvironsci.com

2, 3-(2-alkylthio)-6,7-bis(2-alkylthio)TTF: a new and green synthetic anti-corrosive inhibitors for mild steel in 1.0 HCl

D. Jeroundi [1], S. Chakroune [1], H. Elmsellem [2]*, E.M. El Hadrami [1], A. Ben-Tama [1], A. Elyoussfi [2], A. Dafali [2], C. Douez [3], B. Hafez [4]

[1] *Laboratoire de Chimie Organique Appliquée, Université Sidi Mohamed Ben Abdallah, Faculté des Sciences et Techniques, BP 2202 Fez, Morocco.*
[2]*Laboratoire de chimie analytique appliquée, matériaux et environnement (LC2AME), Faculté des Sciences, B.P. 717, 60000 Oujda, Morocco.*
[3]*Université d'Artois,62000, Arras, France*
[4]*University of Sharjah, department of Chemistry, faculty of science, baraahafez@msn.com , tel:00971554098680*

Received 22 Jun 2016,
Revised 21 Oct 2016,
Accepted 25 Oct 2016

Keywords
- ✓ *TTF,*
- ✓ Corrosion inhibition,
- ✓ Electrochemical studies,
- ✓ DFT,
- ✓ Quantum chemical parameters,

h.elmsellem@gmail.com ;
Phone: +212600254809

Abstract

A new 2,3-(2-alkylthio)-6,7-bis(2-alkylthio)TTF was prepared, characterized by NMR spectroscopy and its anti-corrosion properties were studied and observed. The anticorrosion property of 2,3-(2-alkylthio)-6,7-bis(2-alkylthio)TTF has been studied as a possible source of non-toxic corrosion inhibitor of mild steel in 1M HCl. The techniques included weight loss method, electrochemical measurements, and quantum chemical calculations. Dependence of corrosion inhibition efficiency on various parameters was examined and it was seen that increase in concentration of inhibitor lead to increase in inhibition efficiency. The dipole moment and E_{HOMO}-E_{LUMO} influence the inhibition efficiency which was observed by using quantum chemical studies.

1. Introduction

The chemistry of 1, 3- dithiole ring system has attracted intense interests in various areas of chemistry and new materials science [1] due to the many important properties such as the oxidation to the stable 6 π 1, 3- dithiolium cation, and they also showed a good inhibitory action on the corrosion of metals [2-3]. The ring system is an important organosulfur compound and the planarity of the 1, 3- dithiolium cation aids the formation of close intermolecular interactions in the solid state owing to the good overlapping π-π orbits, besides a large number of functionalities can be incorporated into the 4- and 5- positions. Furthermore, the combination of two rings of 1,3-dithiole-2-thione lead to yield tetrathiafulvalene (TTF) via cross-coupling. TTF and related heterocycles feature unique electron donating capabilities [4] for preparing charge- transfer salts [5], donors- acceptors (D-A) systems and other fields including molecular logic gates [6], molecular switches [7-8], semiconductors [9-10], conductors and superconductors [11-12], organogelators [13], liquid crystals [14-15], dyes absorbing over the whole visible spectrum [16], sensors for proton, cations or anions [17-19], and ligands [20-23].
The aim of the present study is to test the corrosion inhibition efficiency of TTF moiety.

2. Material and Methods

2.1. Synthesis of the inhibitors

Synthesis of 2,3-(propylenedithio)-6,7-bis(2-cyanoethylthio)TTF S1:

A suspension of 4,5- (propylenedithio) -1,3-dithiol-2-thione (1 g, 4.2 mmol) and 4,5- (2-cyanoethylthio) -1,3-dithiol-2-thione (1.3 g, 4.2 mmol) in 25 ml of freshly distilled triethylphosphite is stirred and heated at 100°C for 5h under a nitrogen atmosphere. The mixture is then cooled to 0°C and the precipitate formed is then

filtered, washed with ether and dried under vacuum. Chromatography on a silica column (CH_2Cl_2) of the precipitate makes it possible to isolate the compound **S1** as orange crystals.Yield (71%); mp 188-189°C.
RMN ^{1}H ($CDCl_3$) (δppm):2, 90 (4H, t, SCH_2); 2, 55 (2H,m, CH_2); 2, 75 (4H, t, CH_2CN); 3, 15 (4H, t, SCH_2)**RMN ^{13}C ($CDCl_3$) (δppm):**19,4(2C, CH_2CN);27,1(2C,SCH_2); 31,7(CH_2); 51,4(SCH_2); 117,7(C≡C); 128(=C–S); 129,7(C=C).

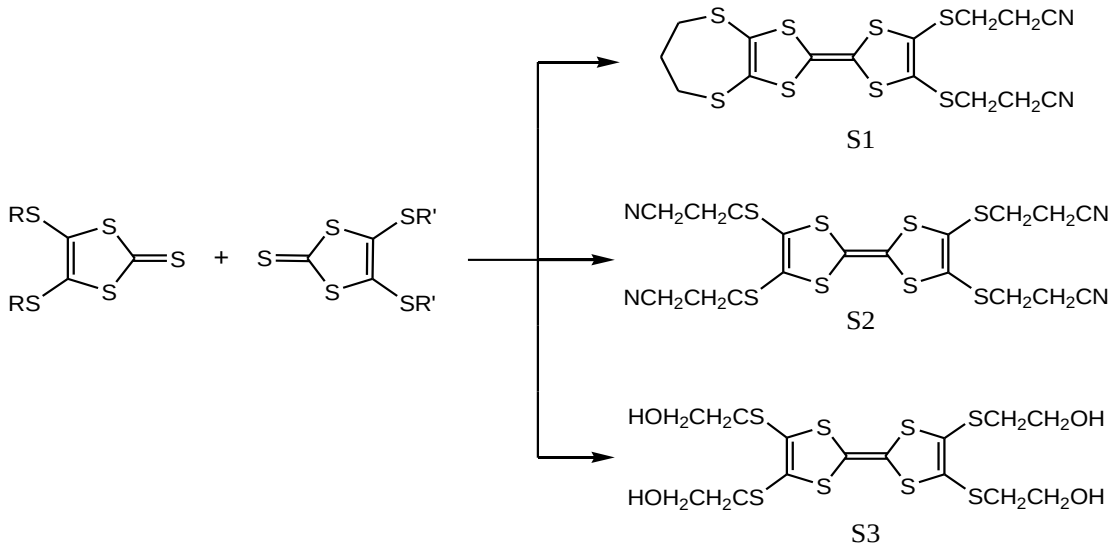

Scheme: *Synthesis of 2,3-(2-alkylthio)-6,7-bis(2-alkylthio)TTF*

Synthesis of 2, 3, 6, 7-Tetrakis (2'-cyanoethylthio)tetrathiafulvalene S2:
4, 5-bi (2-cyanoéthylthio)-1, 3-dithiole-2-thione (1.40 g, 4.85 mmol) was suspended in freshly distilled triethylphosphite (5 mL) and refluxed. After about 30 min a red-orange precipitate starts to form, the red solution was stirred for an additional 1h at reflux and then allowed to cool at room temperature. MeOH (25 mL) was added, the product was filtered, washed with MeOH (3 x 25 mL) and dried *in vacuum*, to give **S2** as intense red-orange crystals. Yield(66%); mp 186-188°C.
RMN ^{1}H ($CDCl_3$) (δ PPM): 2,60 (8H, m, CH_2CN); 3,10 (8H, m, SCH_2)**RMN ^{13}C ($CDCl_3$) (δppm):**19,4(4C, CH_2CN); 51,7(4C, SCH_2); 117,7(C≡N); 128(=C–S); 129,7(C=C).

Synthesis of 2, 3, 6, 7- Tetrakis (2'-hydroxyéthyldithio) tetrathiafulvalene S3:
The same procedure as for the synthesis of compound S2 on 4, 5- (2-hydroxyethyldithio) -1, 3-dithiol-2-thione (2.4 g, 8.3 mmol) to give **S3** as red-orange crystals. Yield (67%); mp 187-188°C.
RMN ^{1}H ($CDCl_3$) (δ PPM):3,06(8H, t, SCH_2); 4,20(8H, m, CH_2OH); 2,04(4H, OH) **RMN ^{13}C ($CDCl_3$) (δppm):**33,8(4C, SCH_2); 61,3(4C, CH_2OH); 128(=C–S); 129,7(C=C).

2.2. Weight loss measurements
Coupons were cut into 1.5× 1.5 × 0.05 cm^3 dimensions having composition (0.09%P, 0.01 % Al, 0.38 % Si, 0.05 % Mn, 0.21 % C, 0.05 % S and Fe balance) used for weight loss measurements. Prior to all measurements, the exposed area was mechanically abraded with 180, 400, 800, 1000, 1200 grades of emery papers. The specimens are washed thoroughly with double distilled water degreased and dried with ethanol. Gravimetric measurements are carried out in a double walled glass cell equipped with a thermostatic cooling condenser. The solution volume is 100 cm^3. The immersion time for the weight loss is 6 h at (308±1) K.

2.4. Electrochemical tests
The electrochemical study was carried out using a potentiostat PGZ100 piloted by Voltamaster soft-ware. This potentiostat is connected to a cell with three electrode thermostats with double wall. A saturated calomel electrode (SCE) and platinum electrode were used as reference and auxiliary electrodes, respectively. Anodic and cathodic potentiodynamic polarization curves were plotted at a polarization scan rate of 0.5mV/s. Before all experiments, the potential was stabilized at free potential during 30 min. The polarisation curves are obtained from −800 mV to −200 mV at 308 K. The solution test is there after de-aerated by bubbling nitrogen. The electrochemical impedance spectroscopy (EIS) measurements are carried out with the electrochemical system,

which included a digital potentiostat model Voltalab PGZ100 computer at Ector after immersion in solution without bubbling. After the determination of steady-state current at a corrosion potential, sine wave voltage (10 mV) peak to peak, at frequencies between 100 kHz and 10 mHz are superimposed on the rest potential. Computer programs automatically controlled the measurements performed at rest potentials after 0.5 hour of exposure at 308 K. The impedance diagrams are given in the Nyquist representation. Experiments are repeated three times to ensure the reproducibility.

2.5. Quantum chemical calculations

Quantum chemistry calculations for the geometrical full optimization of all studied inhibitors were carried out at the density function theory (DFT) method, B3LYP/6-31G level using a GAUSS-09 program package [24]. The following quantum chemical indices were considered: the energy of the highest occupied molecular orbital (E_{HOMO}), the energy of the lowest unoccupied molecular orbital (E_{LUMO}), $\Delta E = E_{LUMO} - E_{HOMO}$, the dipole moment (**μ**), total energy and Fukui induce.

3. Results and discussion

3.1.Weight loss measurements

The inhibition efficiency (η) and corrosion rate (w) with different concentrations of 2,3-(2-alkylthio)-6,7-bis(2-alkylthio)TTF derivatives for mild steel in 1.0 M HCl solution at 308 K were summarized in Table 1. The inhibition efficiency was calculated from the following equation:

$$C_R = \frac{w_b - w_a}{At} \qquad (1)$$

$$\eta(\%) = \left(1 - \frac{w_i}{w_0}\right).100 \qquad (2)$$

Table1: Corrosion rate and inhibition efficiency in the absence and presence of S1, S2 and S3 in 1.0 M HCl solution.

Inhibitor	C (mol/l)	C_R ($mg.cm^{-2} h^{-1}$)	η (%)	θ
1M HCl	--	0.82	--	--
S1	10^{-6}	0.31	62	0.62
	10^{-5}	0.22	73	0.73
	10^{-4}	0.13	84	0.84
	10^{-3}	0.06	93	0.93
S2	10^{-6}	0.39	52	0.52
	10^{-5}	0.32	61	0.61
	10^{-4}	0.19	77	0.77
	10^{-3}	0.11	87	0.87
S3	10^{-6}	0.35	57	0.57
	10^{-5}	0.27	67	0.67
	10^{-4}	0.15	82	0.82
	10^{-3}	0.08	90	0.90

The studied inhibitors showed maximum inhibition efficiencies of 93%, 90% and 87% for S1, S2 and S3, respectively at 10^{-3}M concentration. It can be seen from Tab.1 that after 10^{-3}M, no significant change in the inhibition performance was observed indicating that 10^{-3}M is an optimum concentration in each case. The high

η of investigated TTF molecules is attributed to the presence of S, N and O, which act as an adsorption centers and can effectively cover the metal surface. The higher inhibition efficiency of the S1, S3 as compared to S2 is attributed to the presence of S and OH substituents in S1, S3, respectively.

3.2.Adsorption isotherm

The adsorption isotherm experiments were performed to have more insights into the mechanism of corrosion inhibition, since it describes the molecular interaction of the inhibitor molecules with the active sites on the mild steel surface [25-27]. The surface coverage, θ, was calculated according to the following equation:

$$\theta = {}^{\eta}/_{100} \qquad (3)$$

Basic information on the interaction between inhibitor and metal surface can be provided by the adsorption isotherm. Attempts were made to fit experimental data to various isotherms including Frumkin, Langmuir, Temkin and Freundlich isotherms. By far the results were best fitted by Langmuir adsorption isotherm equation [28]:

$$\frac{C}{\theta} = \frac{1}{K} + C \qquad (4)$$

Where C is the concentration of inhibitor, K the adsorption equilibrium constant, and θ is the surface coverage. Plots of C/θ against C yield straight lines as shown in Fig. 1, and the linear regression parameters are listed in Table.2. Both linear correlation coefficient (r) and slope are very close to 1, indicating the adsorption of both inhibitors on steel surface obeys the Langmuir adsorption isotherm.

Table2: Parameters of the straight line of **C/θ - C** in 1.0 M HCl at 308 K (weight loss method, immersion time is 6 h).

Inhibitors	Linear correlation coefficient (r)	Slope
S1	1	1.18966
S2	0.99996	1.07487
S3	0.99994	1.14907

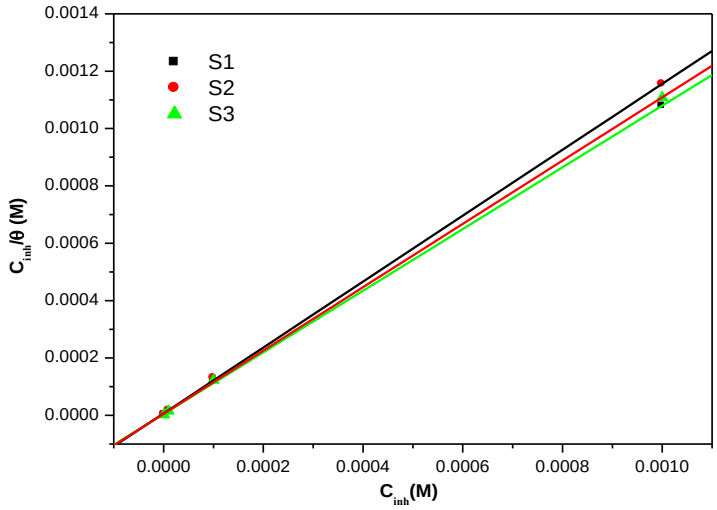

Figure1: Langmuir isotherm plots for adsorption of 2,3-(2-alkylthio)-6,7-bis(2-alkylthio)TTF derivatives S1, S2 and S3 on mild steel in 1.0 M HCl.

3.3.Tafel polarization

Anodic and cathodic polarization curves for mild steel in 1M HCl with and without various concentrations of used inhibitors are shown in Fig. 2. It is observed from Fig. 2 that both cathodic and anodic curves show a lower current density in the presence of S1, S2 and S3 additives than those recorded in the 1M HCl solution alone.
This behavior indicated that these two used S1, S2 and S3 have effect on both cathodic reactions of corrosion process. Polarization curves of the MS electrode in 1.0 M HCl without and with addition of 2,3-(2-alkylthio)-6,7-bis(2-alkylthio)TTF at different concentrations are shown in Fig.2. The values of electrochemical parameters associated with polarization measurements, such as corrosion potential (E_{corr}), corrosion currents densities (I_{corr}) and Tafel slopes (βa, βc) are listed in Table 3. The inhibition efficiencies were calculated from

I_{corr} values (Tab 3) obtained from extrapolating Tafel lines to the corrosion potential [29] according to following equation:

$$\eta(\%) = \frac{Icorr - Icorr(inh)}{Icorr}.100 \qquad (5)$$

Where I_{corr} and $I_{corr(inh)}$ are the corrosion current densities for uninhibited and inhibited solutions, respectively.

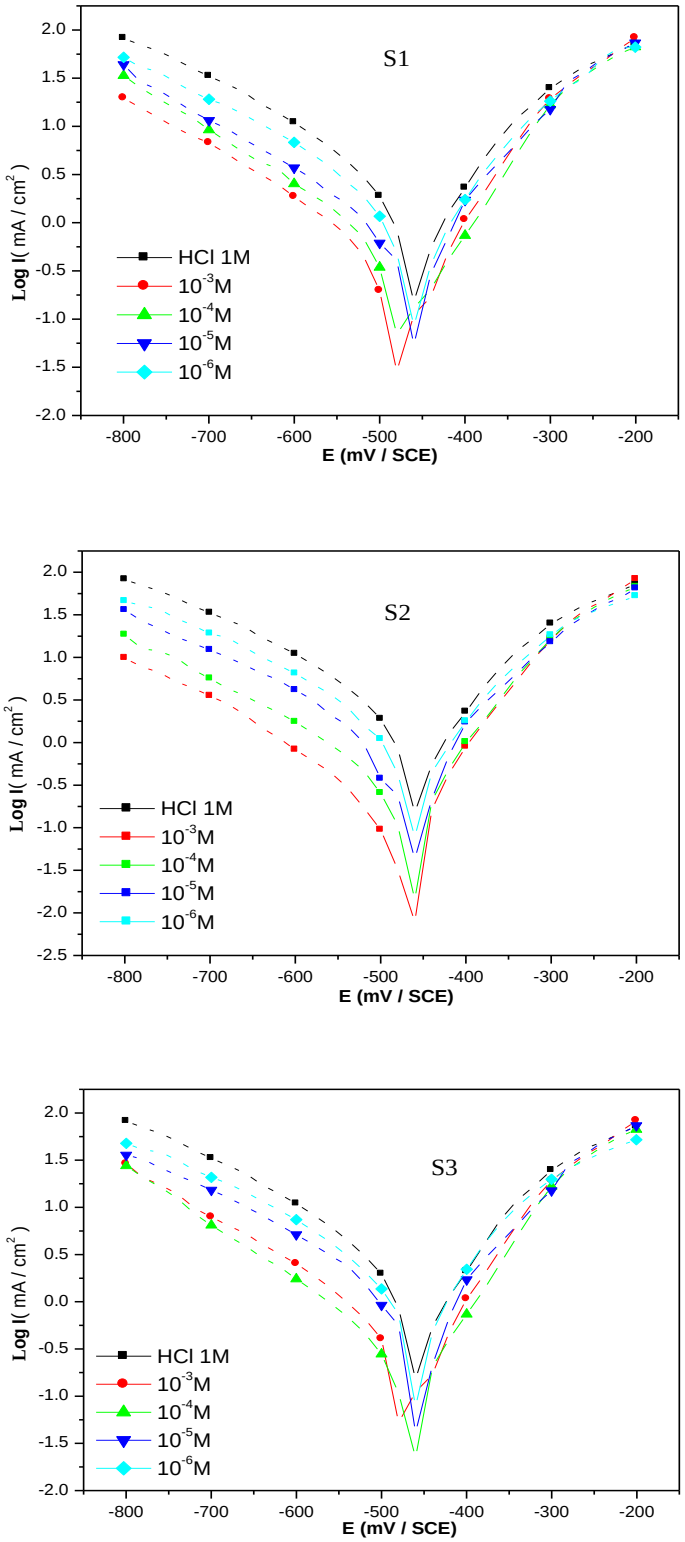

Figure2: Anodic and cathodic potentiodynamic polarization curves for mild steel in 1.0 M HCl without and with different concentration of S1, S2 and S3 at 308K.

As it can be seen from Table 3, when the concentration of inhibitors increases the inhibition efficiencies and also surface coverage degrees increase, but corrosion current densities decrease. From Table 3 also can find that

the corrosion potentials of inhibitors A S1, S2 and S3 shift in the positive direction. The electrochemical processes on the metal surface are likely to be closely related to the adsorption of the inhibitor, and the adsorption is known to depend on the chemical structure of the inhibitor [30]. In hydrochloric acid solution the following mechanism is proposed for the corrosion of iron and steel [31]. According to this mechanism cathodic dissolution of iron is:

$$Fe + H^+ \longleftrightarrow (FeH^+)_{ads} \quad (6)$$

$$(FeH^+)_{ads} + e^- \longrightarrow (FeH)_{ads} \quad (7)$$

$$(FeH)_{ads} + H^+ + e^- \longrightarrow Fe + H_2 \quad (8)$$

The values of cathodic Tafel slope (βc) for three TTF derivatives are found to increase in the presence of inhibitor. The Tafel slope variations suggest that all TTF derivatives influence the kinetics of the hydrogen evolution reaction [32-34]. The approximately constant values of anodic Tafel slope (βa) for TTF derivatives S1, S2 and S3 indicate that these compounds do not change the mechanism of MS dissolution.

Table 3: Polarization parameters and corresponding inhibition efficiency for the corrosion of the mild steel in 1M HCl without and with addition of various concentrations of S1, S2 and S3 at 308K.

Inhibitor	C (mol/L)	$-E_{corr}$ (mV/SCE)	I_{corr} (μA/cm^2)	$-\beta_c$ (μA/cm²)	β_a (μA/cm²)	η (%)
1M HCl	-	453	1386	173	113	--
S1	10^{-6}	491	512	149	87	63
	10^{-5}	479	391	140	62	72
	10^{-4}	487	250	148	95	82
	10^{-3}	467	85	134	68	94
S2	10^{-6}	451	603	151	108	56
	10^{-5}	472	452	163	96	67
	10^{-4}	764	367	149	85	74
	10^{-3}	490	163	168	101	88
S3	10^{-6}	459	571	147	105	59
	10^{-5}	475	444	164	79	68
	10^{-4}	467	316	138	56	77
	10^{-3}	486	141	155	83	90

3.4.Electrochemical impedance spectroscopy (EIS)

The corrosion behavior of MS in 1M HCl in the presence and absence of S1, S2 and S3 compounds has been investigated using EIS at 308K. Nyquist plots of mild steel in acid solutions containing various concentrations of inhibitors S1, S2 and S3 and without inhibitors in the 1M HCl solution are given in Fig. 3. It is clear from the plots that the impedance response of mild steel in 1M HCl solution was significantly changed after the addition of the inhibitor compounds. The charge-transfer resistance (Rt) values are calculated from the difference in impedance at lower and higher frequencies. The double layer capacitance (Cdl) and the frequency at which the imaginary component of the impedance is maximal ($-Z_{max}$) are found as represented in equation:

$$C_{dl} = \left(1/\omega R_t\right) \qquad \text{Where} \qquad \omega = 2\pi f_{max} \quad (9)$$

The inhibition efficiency got from the charge transfer resistance is calculated by:

$$E_z = \left(1 - \frac{R_t}{R_{t/inh}}\right).100 \quad (10)$$

Rt and Rt/inh are the charge transfer-resistance values without and with inhibitor, respectively.

Various parameters such as charge-transfer resistance (Rt), double layer capacitance (Cdl) and f_{max} were obtained from impedance measurements and are shown in Table 4.

From the Table 4, it is clear that as the inhibitors concentration increased, the Rct values increased and the C_{dl} values decreased, which is due to a decrease in local dielectric constant and/or an increase in the thickness of the electrical double layer, suggesting that the inhibitor molecules acted by adsorption at the metal/solution interface [35]. The inhibition performance order of TTF molecules is S1 > S3 > S2. The same trend was obtained from the weight loss and potentiodynamic polarization methods.

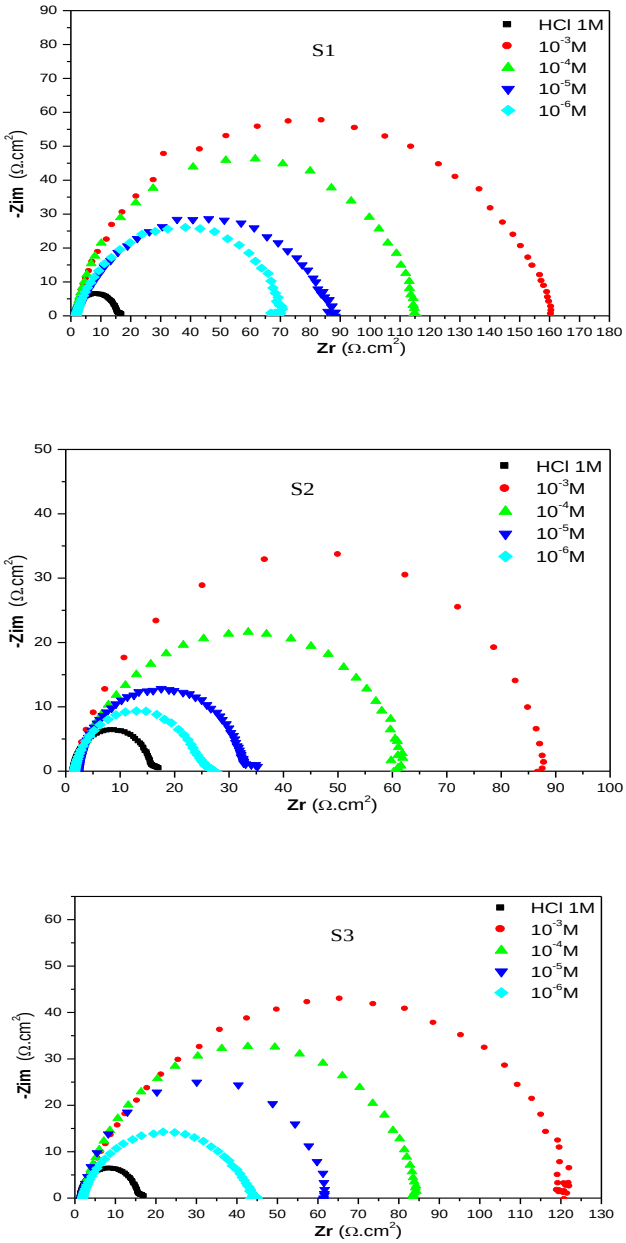

Figure 3: Impedance parameters for MS in 1M HCl for various concentrations of S1, S2 and S3.

Table 4: Impedance parameter values for the corrosion of mild steel in 1M HCl.

Inhibitors	C (mol/l)	R_t ($\Omega.cm^2$)	C($\mu f/cm^2$)	η(%)
1M HCl	-	15	200	--
S1	10^{-6}	70	145	79
	10^{-5}	90	98	83
	10^{-4}	115	60	87
	10^{-3}	160	35	91
S2	10^{-6}	27	179	44
	10^{-5}	35	123	57
	10^{-4}	63	76	76
	10^{-3}	89	51	83
S3	10^{-6}	45	167	67
	10^{-5}	62	111	76
	10^{-4}	84	70	82
	10^{-3}	120	47	88

3.5. Quantum chemical calculations

Quantum chemical calculations are used to correlate experimental data for inhibitors obtained from different techniques (viz., electrochemical and weight loss) and their structural and electronic properties.

Popular qualitative chemical concepts such as electronegativity [36-37] (χ) and hardness [38] (η) have been provided with rigorous definitions within the purview of conceptual density functional theory [39-41] (DFT). Electronegativity is the negative of chemical potential defined [42] as follows for an N-electron system with total energy E and external potential $v(\vec{r})$:

$$\chi = -\mu = -\left(\frac{\partial E}{\partial N}\right)_{v(r)} \qquad (11)$$

μ is the Lagrange multiplier associated with the normalization constraint of DFT [43, 44].

Hardness (η) is defined [45] as the corresponding second derivative:

$$\eta = -\left(\frac{\partial^2 E}{\partial N}\right)_{v(r)} = -\left(\frac{\partial \mu}{\partial N}\right)_{v(r)} \qquad (12)$$

Using a finite difference method, working equations for the calculation of χ and η may be given as [46]:

$$\chi = \frac{I+A}{2} \qquad (13)$$

$$\eta = \frac{I-A}{2} \qquad (14)$$

Where I = -EHOMO and A= -ELUMO are the ionization potential and electron affinity respectively.

The fraction of transferred electrons ΔN was calculated according to Pearson theory [47]. This parameter evaluates the electronic flow in a reaction of two systems with different electronegativity's, in particular case; a metallic surface (Fe) and an inhibitor molecule. ΔN is given as follows:

$$\Delta N = \frac{\chi_{Fe} - \chi_{inh}}{2(\eta_{Fe} + \eta_{inh})} \qquad (15)$$

where χFe and χinh denote the absolute electronegativity of an iron atom (Fe) and the inhibitor molecule, respectively; ηFe and ηinh denote the absolute hardness of Fe atom and the inhibitor molecule, respectively.

In order to apply the eq. 12 in the present study, a theoretical value for the electronegativity of bulk iron was used χFe = 7 eV and a global hardness of ηFe = 0, by assuming that for a metallic bulk I = A because they are softer than the neutral metallic atoms [48].

The electrophilicity has been introduced by Parr et al. [49], is a descriptor of reactivity that allows a quantitative classification of the global electrophilic nature of a compound within a relative scale. They have proposed the ω as a measure of energy lowering owing to maximal electron flow between donor and acceptor and ω is defined as follows:

$$\omega = \frac{\chi^2}{2\eta} \qquad (16)$$

The Softness σ is defined as the inverse of the η [50]:

$$\sigma = \frac{1}{\eta} \qquad (17)$$

The FMOs (HOMO and LUMO) are very important for describing chemical reactivity. The HOMO containing electrons, represents the ability (EHOMO) to donate an electron, whereas, LUMO haven't not electrons, as an electron acceptor represents the ability (ELUMO) to obtain an electron. The energy gap between HOMO and LUMO determines the kinetic stability, chemical reactivity, optical polarizability and chemical hardness–softness of a compound [51].

Firstly, in this study, we calculated the HOMO and LUMO orbital energies by using B3LYP method with 6-31G. All other calculations were performed using the results with some assumptions. The higher values of EHOMO indicate an increase for the electron donor and this means a better inhibitory activity with increasing adsorption of the inhibitor on a metal surface, whereas ELUMO indicates the ability to accept electron of the molecule. The adsorption ability of the inhibitor to the metal surface increases with increasing of EHOMO and decreasing of ELUMO. The HOMO and LUMO orbital energies and image of P1 were performed and were shown in Table 5 and Figure 5.

High ionization energy (I= 6. 06 eV, I= 6.13 and 6.41 for S1, S2 and S3 respectively) indicates high stability of inhibitor, the number of electrons transferred (ΔN) was also calculated and tabulated in Table 5. The ΔN < 1.6 indicates the tendency of a molecule to donate electrons to the metal surface.

Table 5: Quantum chemical parameters for S1-S3 obtained in gas phase with the DFT at the B3LYP/6-31G level.

Prameters	Phase		
	S1	S2	S3
Total Energy TE (eV)	-60486.7	-65662.1	-66588.7
EHOMO (eV)	-6.0621	-6.1277	-6.4085
ELUMO (eV)	-3.2568	-3.4108	-3.6802
Gap ΔE (eV)	2.8054	2.7169	2.7283
Dipole moment μ (Debye)	6.7078	5.9814	5.4165
Ionisation potential I (eV)	6.0621	6.1277	6.4085
Electron affinity A	3.2568	3.4108	3.6802
Electronegativity χ	4.6594	4.7692	5.0443
Hardness η	1.4027	1.3585	1.3642
Electrophilicity index ω	7.7389	8.3718	9.3262
Softness σ	0.7129	0.7361	0.7330
Fractions of electron transferred ΔN	0.8343	0.8211	0.7168

Table 6 : The HOMO and the LUMO electrons density distributions of the studied inhibitors computed at B3LYP/6-31G level in gas phase.

	HOMO	LUMO
P1	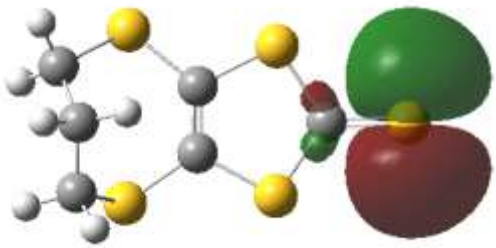	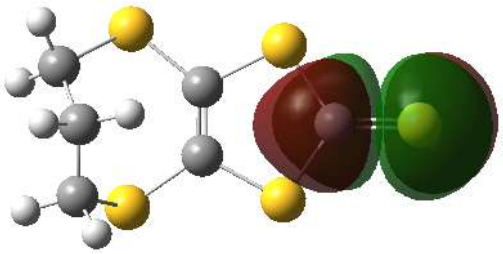
P2	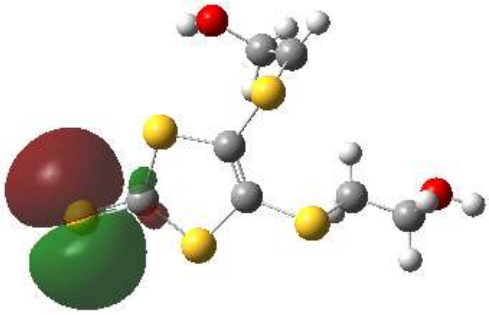	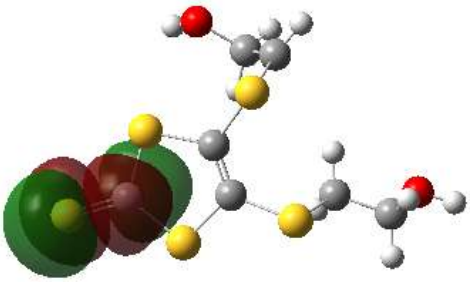
P3	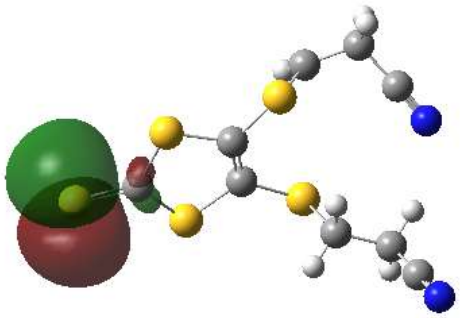	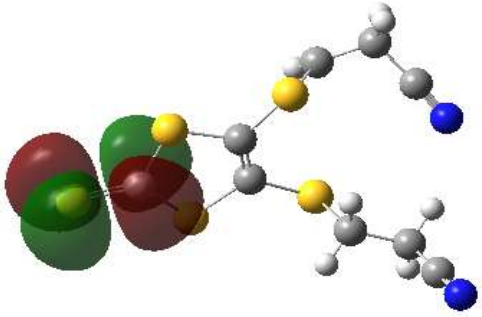

Conclusion

- The inhibition efficiency follows the order S1 >S3> S2 in all methods employed with small differences in their numerical values.
- Both 2,3-(2-alkylthio)-6,7-bis(2-alkylthio)TTF derivatives S1, S2 and S3 are good inhibitors for mild steel corrosion in hydrochloric acid solution, generating inhibition efficiencies in the order of S1 >S3> S2 at concentration of 10^{-3} mol/l.
- Adsorption of the TTF derivatives on the mild steel surface obeys the Langmuir's isotherm.
- The results obtained from the potentiodynamic polarization indicate that these 2,3-(2-alkylthio)-6,7-bis(2-alkylthio)TTF act as cathodic-type inhibitors.
- Quantum chemical approach is adequately sufficient to also forecast the inhibitor effectiveness using the theoretical approach. However, it may be used to find the optimal group of parameters that might predict the structure and molecule suitability to be an inhibitor.

References

1. T. K. Hansen, J. Becher, *Adv. Mater*. 5(1993) 288.
2. D. Jeroundi, H. Elmsellem, S. Chakroune, R. Idouhli, A. Elyoussfi, A. Dafali, E. M. El Hadrami, A. Ben-Tama, Y. Kandri Rodi, *J. Mater. Environ. Sci. 7 (11) (2016) 4024-4035.*
3. D. Jeroundi, H. Elmsellem, S. Chakroune, B. Hammouti, R. Idouhli, E. M. El Hadrami, A. Ben-Tama, M. Oudani, Y. Ouzidan and Y. Kandri Rodi, *J. Mater. Environ. Sci.* 7 (10) (2016) 3895-3905.
4. R. Chadli, M. Elazouzi,I. Khelladi, A.M. Elhourri, H. Elmsellem, A. Aouniti, J. Kajima Mulengi, B. Hammouti. Portugaliae Electrochimica Acta. 35(2017)65-80
5. X. Shao, Y. Yamaji, T. Sugimoto, H. Tanaka, *Chem Mater*. 21(2009) 5569.
6. E.H. Witlick, C. Johnsen, S.W. Hansen, D.W. Silverstein, V.J. Bottomley, J.O. Jeppesen, E.W. Wong, L. Jensen, A.H. Flood, J. Am. Chem. Soc. 133 (2011)7288–7291.
7. C. Simão, M. Mas-Torrent, J. Casado-Montenegro, F. Otón, J. Veciana, C. Rovira, J Am. Chem. Soc. 133 (2011) 13256–13259.
8. L. Jia, G. Zhang, D. Zhang, J. Xiang, W. Xu, D. Zhu, Chem. Commun. 47 (2011) 322–324.
9. F. Otón, R. Pfattner, E. Pavlica, Y. Olivier, E. Moreno, J. Puigdollers, G. Bratina,J. Cornil, X. Fontrodona, M. Mas-Torrent, J. Veciana, C. Rovira, Chem. Mater. 23 (2011) 851–861.
10. F. Otón, R. Pfattner, N.S. Oxtoby, M. Mas-Torrent, K. Wurst, X. Fontrodona,Y. Olivier, J. Cornil, J. Veciana, C. Rovira, J. Org. Chem. 76 (2011) 154–163.
11. Special issue on molecular conductors: *Chem. Rev*. 104 (2004) 4887; Batail, P., Ed.
12. TTF Chemistry: Fundamentals and Applications of Tetrathiafulvalene; Yamada, J., Sugimoto, T., Eds.; Springer: Berlin, 2004.
13. X.-J. Wang, L.-B. Xing, W.-N. Cao, X.-B. Li, B. Chen, C.-H. Tung, L.-Z. Wu, *Langmuir* 27 (2011) 774–781.
14. L. Wang, H. Cho, S.-H. Lee, C. Lee, K.-U. Jeong, M.-H. Lee, *J. Mater. Chem.* 21 (2011) 60–64.
15. R. Hou, K. Zhong, Z. Huang, L.Y. Jin, B. Yin, *Tetrahedron*. 67 (2011) 1238–1244.
16. P.-A. Bouit, C. Villegas, J.L. Delgado, P.M. Viruela, R. Pou-Amérigo, E. Ortí, N. Martín, *Org. Lett*. 13 (2011) 604–607.
17. Z. Shi, Q.-H. Han, X.-Y. Li, M.-Y. Shao, Q.-Y. Zhu, J. Dai, *Dalton Trans*. 40 (2011) 7340–7347.
18. M.H. Lee, Q.-Y. Cao, S.K. Kim, J.L. Sessler, J.S. Kim, *J. Org. Chem*. 76 (2011) 870–874.
19. K. Flídrová, M. Tkadlecová, K. Lang, P. Lhoták, *Dyes Pigments*. 92 (2011) 668–673.
20. J. Qin, L. Hu, G.-N. Li, X.-S. Wang, Y. Xu, J.-L. Zuo, X.-Z. You, *Organometallics*. 30 (2011) 2173–2179.
21. M. Guerro, T.U. Dam, S. Bakhta, B. Kolli, T. Roisnel, D. Lorcy, *Tetrahedron*. 67(2011) 3427–3433.
22. Y. Wang, B. Li, G. Huang, J.-P. Zhang, Y. Zhang, *New J. Chem*. 35 (2011) 1472–1476.
23. G.-N. Li, D. Wen, T. Jin, Y. Liao, J.-L. Zuo, X.-Z. You, Tetrahedron Lett. 52 (2011) 675–678.
24. L. Essaghouani, H. Elmsellem, M. Ellouz, M. El Hafi, M. Boulhaoua, N. K. Sebbar, E. M. Essassi, M. Bouabdellaoui, A. Aouniti and B. Hammouti , *Der Pharma Chemica*. 8 (2016) 297-305.
25. M. Lebrini, F. Bentiss, N. Chihib, C. Jama, J.P. Hornez, M. Lagrenée, *Corros. Sci*. 50 (2008) 2914.

26. A. Elyoussfi, A. Dafali, H. Elmsellem, H. Steli, Y. Bouzian, K. Cherrak, Y. El Ouadi, A. Zarrouk, B. Hammouti, J. Mater. Environ. Sci. 7 (2016) 3344.
27. D.A. Lopez, S.N. Simison, S.R. deSanchez, *Electrochim. Acta* 48 (2003) 845.
28. M. Lebrini, F. Bentiss, N. Chihib, C. Jama, J.P. Hornez, M. Lagrenée, *Corros. Sci*. 50 (2008) 2914.
29. A.K. Singh, M.A. Quraishi, *Corros. Sci*. 53 (2011) 1288.
30. F. Xu, J. Duan, S. Zhang, & B. Hou, *Materials Letters*, 62 (2008) 4072-4074.
31. C. Kustu, K. C. Emregul, O. Atakol, *Corros. Sci*. 49 (2007) 2800- 2814.
32. H. Elmsellem, H. Nacer, F. Halaimia, A. Aouniti,I. Lakehal, A. Chetouani, B. Hammouti, *Int. J. Electrochem. Sci. 9*(2014) 5328-5351.
33. W. Li, Q.He, C. Pei, B.Hou, *Electrochim. Acta.* 52 (2007) 6386-6394.
34. H. Elmsellem,N. Basbas, A. Chetouani, A. Aouniti, S. Radi, M. Messali, B. Hammouti, *Portugaliae Electrochimica Acta, 32*(2014) 77-108.
35. A. Elyoussfi, H. Elmsellem , A. Dafali, K. Cherrak, A. Zarrouk ,B. Hammouti , *Der Pharma Chemica.* 7 (2015) 284-291.
36. H. Elmsellem, T. Harit, A. Aouniti, F. Malek , A. Riahi, A. Chetouani, B. Hammouti, *Protection of Metals and Physical Chemistry of Surfaces.* 51 (2015) 873.
37. K.D. Sen, C. Jorgenson, Structure and bonding: electronegativity, vol. 66 (Springer, Berlin, 1987)
38. K.D. Sen, D.M.P. Mingos, Structure and bonding: chemical hardness, vol. 80 (Springer, Berlin, 1993).
39. R.G. Parr, W. Yang, Density functional theory of atoms and molecules (Oxford University Press, Oxford, 1989).
40. P. Geerlings, F. de Proft, W. Langenaeker, *Chem. Rev*. 103 (2003) 1793.
41. H. Chermette, *J. Comput. Chem*. 20 (1999) 129.
42. R.G. Parr, R.A. Donnelly, M. Levy, W. Palke, *J. Chem. Phys*. 68 (1978) 3801.
43. H. Bendaha, H. Elmsellem , A. Aouniti , A. Chetouani , B. Hammouti, *Physicochemical Mechanics of Materials.*, 1 (2016) 111-118.
44. W. Kohn, L. Sham, *J. Phys. Rev. A.* 140 (1965) 1133.
45. R.G. Parr, R.G. Pearson, *J. Am. Chem. Soc.*105 (1983)7512.
46. R.K. Roy, S. Pal, K. Hirao, *J. Chem. Phys*.110 (1999) 8236.
47. R. Chadli, A. ELherri, H. Elmsellem, M. Elazzouzi, N. Merad, A. Aouniti, B. Hammouti, J. K. Mulengi and A. Zarrouk. *Protection of Metals and Physical Chemistry of Surfaces*. 53 (2017) 928–936.
48. V.S. Sastri, *J.R.* Perumareddi. *Corrosion*. 53 (1997) 671.
49. P. Udhayakala, T. V. Rajendiran, and S. Gunasekaran, *Journal of Chemical, Biological and Physical Sciences A*, 2 (2012)1151-1165.
50. M. Govindarajan, M. Karabacak, *Spectrochim Acta Part A Mol Biomol Spectrosc*. 85 (2012) 251–60

(2018) ; http://www.jmaterenvironsci.com